LA-UR-16-26053 (Accepted Manuscript)

Tracking Radionuclide Fractionation in the First Atomic Explosion Using Stable Elements

Bonamici, Chloe Elizabeth
Kinman, William Scott
Hervig, Richard

To be published in: Analytical Chemistry

DOI to publisher's version: 10.1021/acs.analchem.7b01965

Permalink to record: http://permalink.lanl.gov/object/view?what=info:lanl-repo/lareport/LA-UR-16-26053

Tracking radionuclide fractionation in the first atomic explosion using stable elements

Chloë E. Bonamici[11]*, Richard L. Hervig[2], William S. Kinman[1]

[1]Nuclear and Radiochemistry Group, Chemistry Division, Los Alamos National Laboratory, PO Box 1663, MS J514, Los Alamos, NM, 87545, USA

[2]School of Earth and Space Exploration, Arizona State University, PO Box 871404, Tempe, AZ, 85287, USA

Abstract: Compositional analysis of post-detonation fallout is a tool for forensic identification of nuclear devices. However, the relationship between device composition and fallout composition is difficult to interpret because of the complex combination of physical mixing, nuclear reactions, and chemical fractionations that occur in the chaotic nuclear fireball. Using a combination of in situ microanalytical techniques – electron microprobe analysis and secondary ion mass spectrometry – we show that some heavy stable elements (Rb, Sr, Zr, Ba, Cs, Ba, La, Ce, Nd, Sm, Dy, Lu, U, Th) in glassy fallout from the first nuclear test, Trinity, are reliable chemical proxies for radionuclides generated during the explosion. Stable-element proxies show that radionuclides from the Trinity device were chemically, but not isotopically, fractionated by condensation. Furthermore, stable-element proxies delineate chemical fractionation trends that can be used to connect present-day fallout composition to past fireball composition. Stable-element proxies therefore offer a novel approach for elucidating the phenomenology of the nuclear fireball as it relates to the formation of debris and the fixation of device materials within debris.

Compositional analysis of post-detonation residue is a tool for forensic identification of nuclear devices and is widely used as a deterrent to nuclear proliferation[1,2]. In the case of an unattributed, near-surface nuclear explosion, glassy fallout debris will be one of the first and most abundant materials available for investigation of device origin[3]. However, the exact relationship between device composition and fallout composition has remained elusive for more than 50 years[4-13]. A nuclear chain reaction and the resultant explosion transforms, mixes, and fractionates the chemical and isotopic constituents of a device, along with material from the detonation site, in a chaotic fireball.

Pieces of macroscopic fallout debris from near-surface nuclear tests are compositionally and texturally heterogeneous agglomerations of glass, mineral fragments[1,10,12,14,15], and, in some cases, metallic spheroids[14], that were assembled progressively within the nuclear fireball (Fig. 1). Glasses, representing frozen droplets of molten ground and device material, are the main reservoir for radionuclides in fallout debris[1,2,4,7,9,12,15] (Fig. 1). The extremely short time span over which materials remain molten (given the high rate of cooling) inhibits compositional modification of the melts through processes like melt mixing or diffusion[3,15]. Thus, each piece of

[1] Current address: Department of Earth and Environmental Science, New Mexico Institute of Mining and Technology, 801 Leroy Place, Socorro, NM, 87801, USA

debris represents multiple samplings of the fireball, and the compositional variability of the glasses preserves the compositional variability, temporal and spatial, within the fireball.

Chemical volatility is the primary control on the incorporation of device-derived material into glassy debris[4-13,16,17]. Reconstruction of device composition therefore requires knowledge of element volatilities and associated element fractionations, which cannot be measured during a nuclear detonation. Volatility and fractionation have been inferred from the abundances of fissionogenic isotopes in bulk fallout samples[1,4,6,8,10,12,14,15,18]. This approach is complicated by other, non-volatility-controlled phenomena that can alter the abundances and ratios of radionuclides, including i) nuclear reactions within the fireball, ii) continued radioactive decay following incorporation into debris, and iii) analytical averaging of compositionally heterogeneous samples during bulk analysis.

A major goal of nuclear forensics studies is measurement of fissionogenic nuclides in microscopic domains of fallout debris. Currently, a combination of instrument sensitivity limitations and mass interferences largely precludes accurate and precise measurement of non-actinide fissionogenic radionuclides by small-volume, in situ mass spectrometry techniques[9,10,14,19]. Accordingly, the purpose of the current contribution is to test whether more abundant, non-fissionogenic, natural trace elements are suitable measurement proxies for fissionogenic radionuclides. This requires establishing that 1) trace element concentrations in fallout debris are volatility controlled, similar to concentrations of device-derived fissionogenic radionuclides, and 2) stable and fissionogenic isotopes of the same element do not undergo mass-dependent fractionation in the fireball.

Experimental Section

Experimental Design

Recent work has shown that as much as 50-60 volume % of the glass within macroscopic Trinity fallout formed as liquid condensed from the fireball plasma[15], as opposed to melting of local sediment. Thus, both the major-element and the radionuclide compositions of certain glasses are controlled by chemical volatility[15]. The major-element compositions of condensates that formed over a range of pressure and temperature conditions can be determined by multiple, spatially resolved chemical analyses of micrometer-scale glass domains within agglomerated pieces of debris. Volatility trends can be assessed by broadly grouping major elements based on relative volatilities – refractory (Al, Ca), transitional (Fe, Mg, Si), and volatile (Na, K) elements[20-22]. Trinity glass compositions within this ternary volatility space define a linear trend (Fig. S-1) that allows for calculation of a simple volatility index – the ratio of volatile to refractory major elements in a given glass domain (Experimental Methods). Assuming rapid, monotonic cooling of the fireball [23], the volatility index also defines a relative timescale, with refractory-element-rich condensates representing early, higher-temperature state of the fireball, and increasingly volatile-element-enriched condensates representing later, lower temperature conditions.

We hypothesize that if volatility controlled the abundances of both ground-derived and device-derived elements in debris, then radionuclide abundances should covary with the major-element volatility index. In light of the fine-scale compositional heterogeneity of fallout debris (Fig. 1), a direct test of this hypothesis requires measurement of device-derived radionuclide abundances and major-element abundances in the same sample volume – i.e., in small glass domains of $< 100\ \mu m^3$. However, most long-lived radionuclides that originated with the nuclear device are present in fallout glass in trace or ultratrace concentrations (ppt-ppb)[24]. On the other

hand, naturally occurring, stable isotopes of the same elements derived from ground material may be incorporated into fallout debris in much higher concentrations (up to 1000 ppm). Providing that there is little or no mass-dependent fractionation of isotopes in the fireball, higher-abundance, stable isotopes can be used as chemical proxies for lower-abundance, fissiongenic isotopes.

Experimental Methods

Major-element analysis

Major elements were measured by electron microprobe (EPMA) point analysis. Details of the analytical methods and measurements are available in Bonamici et al.[15].

The linearity of the CaMgFe glass trend in ternary major-element volatility space (Fig. S-1) allows for calculation of the major-element volatility index (where abundances are in oxide weight %):

$$Volatility\ Index = \frac{Na + K}{Al + Ca + Ti}$$

Trace-element analysis

Trace element analyses (Table S-1) were performed in the Secondary Ion Mass Spectrometry Lab (SIMS) at Arizona State University on a Cameca IMS 6f instrument, using a 10-nA O^- primary beam current impacting the sample at ~21.5 keV and 9-kV accelerating voltage at the sample surface. A 75-eV energy offset at the sample holder was employed to suppress molecular ion interferences [25]. ^{30}Si, ^{85}Rb, ^{88}Sr, ^{90}Zr, ^{98}Mo, ^{133}Cs, ^{138}Ba, ^{139}La, ^{140}Ce, ^{144}Nd, ^{147}Sm, ^{159}Tb, ^{162}Dy, ^{175}Lu, ^{180}Hf, ^{232}Th, and ^{238}U counts were collected in serial on a single electron multiplier by magnetic field switching. On-peak count times were one second for ^{30}Si; four seconds for ^{85}Rb, ^{88}Sr, and ^{139}Ba; eight seconds for ^{90}Zr, ^{133}Cs, ^{139}La, ^{140}Ce, ^{144}Nd, ^{147}Sm, ^{159}Tb, ^{162}Dy, ^{175}Lu, ^{180}Hf, ^{232}Th, and ^{238}U; twelve seconds for ^{147}Sm; and sixteen seconds for ^{98}Mo. Total time for each measurement, including wait times between cycles and magnet jumps, was 23 minutes. The transfer optics were set for a 75-µm maximum area, with a 750-µm circular field aperture inserted to restrict the analyzed area to 30 µm in diameter. Effective MRP was 800. Raw trace element data are recorded as trace-element/^{30}Si ratios.

NIST 611 trace-element glass was used as a running standard. The known trace-element concentrations[26] and measured trace-element/^{30}Si ratio in NIST 611 standard glass were used to calibrate measured trace-element/^{30}Si ratios in unknown trinitite glasses. Ratios were converted to total trace element concentrations using the EPMA-measured SiO_2 weight percent at the SIMS measurement location and the natural isotopic abundance of the measured isotope. Most reported 2σ uncertainties are calculated from the 2SD-percent of the NIST 611 measurements made on a given SIMS mount during a specific analysis session. The detection limit for trace elements was conservatively estimated at 100 ppb (0.10 ppm), based on SIMS ion-yield calculations [25]; thus, in a few cases where measured trace-element concentrations were small and the 2SD-percent calculation gave uncertainties of <0.10 ppm, the uncertainty was fixed at 0.10 ppm.

Uranium and plutonium isotope analysis

U-isotope and ^{239}Pu analyses (Table S-2) were performed in the LANL SIMS lab on a Cameca IMS-1280 large-geometry SIMS, using a 30-nA O^- primary beam. The primary beam

was accelerated to -13 keV from the duoplasmatron source and impacted the sample surface (held at +10 keV) at 23 kV. Measurements are made with an unrastered Gaussian-focused beam and pre-sputtering times of 90 seconds. Transfer-section optics were tuned for 80-μm maximum area (100x magnification of the crossover in the field aperture plane). ^{235}U, ^{238}U and ^{239}Pu counts were measured simultaneously by multicollector with an exit-slit MRP of 2200. Initial peak centering was performed by manual mass scans before each analysis session and updated by automated mass scans on the ^{238}U peak position before each new analysis. NMR control was utilized for magnet stabilization during each analysis. Multicollector electron multipliers were calibrated for yield following final detector trolley positioning and immediately prior to the start of analysis during each analytical session. Ion counts were integrated over 420 four-second counting cycles. Total analysis time for each measurement, including wait time between cycles, was 32 min.

NIST 611 (475 ppm U) and NIST 612 (38 ppm U)[27] were utilized as tuning and analytical standards, with all uncertainty calculations based on sample-bracketing measurements of NIST 612, which has element concentrations most similar to those in Trinity glass samples. $^{235}U/^{238}U$ and $^{239}Pu/^{238}U$ in unknown trinitite glasses were corrected for SIMS instrumental mass fractionation using ratios measured in NIST 612[28,29]:

$$\left(\frac{^{23x}U}{^{238}U}\right)_{corr} = \left[\frac{1+\left(\frac{^{23x}U}{^{238}U}\right)_{meas}^{unk}}{\alpha_{SIMS}}\right] - 1, \text{ where } \alpha_{SIMS} = \left[\frac{1+\left(\frac{^{23x}U}{^{238}U}\right)_{meas}^{NIST612}}{1+\left(\frac{^{23x}U}{^{238}U}\right)_{bulk}^{NIST612}}\right].$$

Bulk values for NIST61x U-isotope ratios are taken from Zimmer et al.[30]. Counts collected at mass 239 were assumed to represent combined counts for ^{239}Pu and the polyatomic $^{238}U^{1}H$ interference (Table S-2). Bias arising from this interference was corrected assuming that all counts at mass 239 in the Pu-free NIST612 were due to hydride formation, and thus that $^{239}Pu/^{238}U$ in NIST 612 is zero. Lastly, $^{235}U/^{238}U$ ratios were corrected for ingrowth of ^{235}U from alpha decay of ^{239}Pu in the 70 years between the time of the Trinity test and the time of SIMS isotope measurements according to

$$\left(\frac{^{235}U}{^{238}U}\right)_{total} - \left(\frac{^{235}U}{^{238}U}\right)_{ingrowth} = \left(\frac{^{235}U}{^{238}U}\right)_{total} - \frac{^{239}Pu}{^{238}U}\left(e^{\lambda t} - 1\right),$$

where $\lambda = 2.875 \times 10^{-5}$ yr^{-1} (^{239}Pu half-life of 24110 years).

Condensation Models

The condensation of a trace element from a vapor or plasma will be a function of the fraction of melt condensed and trace-element partitioning (fractionation) between vapor/plasma and melt. While the exact fractionation relationship is not known, the fractionation behavior can be constrained by comparison with two endmember condensation models (Fig. 2, lower left). The equilibrium model represents the case where the trace element concentration in the condensate is determined by thermodynamic equilibrium partitioning between melt and vapor/plasma. Equilibrium condensation is modeled as:

$$\frac{C_m}{C_0} = \frac{a}{F + aX}$$

The kinetic (Rayleigh) model simulates the case in which the instantaneous partitioning of a trace element between plasma and condensed melt is determined by thermodynamic

equilibrium, but the condensate is immediately isolated from the plasma and cannot maintain equilibrium. Kinetic condensation is modeled as:

$$\frac{C_m}{C_0} = aF^{(a-1)}$$

In both endmember models, variables are defined as follows.

$$\frac{C_m}{C_0} = trace\ element\ concentration\ in\ melt\ to\ element\ concentration\ in\ plasma$$
$$F = fraction\ of\ plasma\ remaining$$
$$X = 1 - F = fraction\ of\ condensed\ melt$$
$$a = \frac{C_m}{C_0}\ at\ equilibrium$$

A trace element having $a > 1$ preferentially concentrates in the condensed melt relative to the plasma, and vice versa for $a < 1$.

Results

We measured major elements, a suite of stable trace elements, and U-Pu isotope ratios at fifty-one spatially resolved locations across nine pieces of Trinity glassy fallout debris (Experimental Methods; Tables S-1 and S-2). Volatility at the time of melt condensation was determined for each analysis location by calculation of the volatility index from major-element composition. In addition, we calculated the volatility index for ~100 previously published Trinity glass analyses that paired spatially resolved trace- and major-element measurements [10]. The calculated volatility indices show that Trinity debris surveyed here preserves condensates formed over a volatility range spanning more than two orders of magnitude. When trace-element concentrations are plotted as a function of volatility index, the data define increasing or decreasing trends that are consistent with their expected volatility behavior (Fig. 2). Concentrations of elements that are usually classified as volatile – Rb, Cs – increase with increasing volatility index, whereas concentrations of elements that are usually considered refractory – Zr, Hf, REEs, U, and Th – decrease with increasing volatility index. Moreover, Cs and Rb show trends consistent with kinetic fraction of incompatible (volatile) elements, whereas Sr, Ba, Zr, Hf, REEs, U, and Th show trends consistent with equilibrium fractionation of compatible (refractory) elements (Fig. 2; Experimental Methods). Trace-element ratio trends indicate the direction and extent of fractionation of the elements with cooling and progressive condensation (Fig. 3). Zr/Hf is nearly uniform over the sampled volatility range, indicating little or no fractionation, whereas Rb/Sr displays a positive trend consistent with concentration of Sr in earlier condensates and Rb in later condensates. Furthermore, the slope of the trace-element-ratio trend should be proportional to the magnitude of fractionation. Thus, the steep Rb/Sr trend indicates large fractionation over the volatility range, whereas the more gradual $^{239}Pu/^{238}U$ trend indicates moderate fractionation of Pu and U.

Within uncertainty, almost all ^{239}Pu-decay-corrected $^{235}U/^{238}U$ ratios are indistinguishable from the natural $^{235}U/^{238}U$ ratio of 0.00725[31] (Fig. 4). The $^{235}U/^{238}U$ ratios show no systematic variation with glass composition or calculated volatility index.

Discussion

Monotonic variations of trace-element concentration with major-element volatility index (Fig. 2) indicate that volatility is a significant control on the incorporation of natural, non-fissionogenic trace elements into glassy fallout debris. Previous work on Trinity glasses invokes a formation mechanism in which minerals in the Trinity site sediment melt. Chemically diverse liquids produced from melting different proportions of these minerals are then physically mixed to produce the range of glass compositions observed[9,10,14,32]. The monotonic trace-element trends documented in this study (Fig. 2) could be generated by binary mixing between two melts with different, and largely fixed, trace-element concentrations. However, binary mixing between two well-defined reservoirs is unlikely because most (if not all) of the natural trace elements measured in this study are sourced from more than one of the test site minerals – e.g., K-feldspar (Rb, Cs, Ba, REEs), calcite (Sr, U), plagioclase (Sr, Ba, REEs), zircon (U, Th, Zr, Hf, REEs), pyroxene (REEs), amphibole (Ba, Mo, REEs), apatite (Sr, U, Th), titanite (U, Th, Zr, Hf, REEs), and Fe-Ti oxides (Mo). Local, variable mixing of different proportions of molten minerals is thus unlikely to produce a unidirectional change in trace-element concentration from a sampling of multiple glass compositions. Progressive fractionation of elements, reflecting progressive, unidirectional change in volatility with cooling from a more uniform plasma/vapor is a more reasonable mechanism to generate monotonic trace-element trends.

Comparison of trace-element ratios allows for determination of relative element volatilities (Fig. 3), which reflect the specific conditions within and environmental composition of the Trinity fireball. Notably, the condensation order inferred by these relative volatilities differs significantly from that inferred from simple metal and metal oxide vaporization experiments [33-35] (Fig. S-2), which have been invoked by previous workers to interpret debris volatility[5,8,11,34]. Rather, the inferred condensation order (though not necessarily absolute condensation temperature) is closer to predictions for condensation order of rocky materials in the early solar system[20,36,37].

Curved and stepped trace-element ratio trends – e.g., Sr/Lu (Fig. 3) – suggest apparent changes in volatility over time. Pressure variation in the fireball is unlikely to produce large differential variations in element volatility (i.e., trace-element ratios) because the magnitude and direction of a pressure effect would be similar for most vaporized elements. Instead, apparent volatility variations may reflect post-condensation, differential ingrowth at some masses by isobaric decay of especially abundant fissionogenic elements. Many condensates form in ≤10 seconds following a nuclear detonation [8,15,17], and thus most fissionogenic nuclides are incorporated into condensing melt as short-lived radioactive precursors that are chemically distinct from, but isobaric with respect to, naturally occurring stable isotopes. The abundance measured at each mass would represent a combination of the natural mass abundance and a smaller fissionogenic addition to that mass. Differences in fission yields and decay-chain element sequences would cause differential fissionogenic additions to the various masses, and thus could cause apparent variations in relative volatilities as represented by trace-element ratios.

The volatility index can be used to independently test the assumption of little or no mass-dependent isotopic fractionation (of heavy elements) during a nuclear detonation. Uranium in Trinity fallout glass reflects a combination of uranium derived from the Trinity device tamper [38] and naturally occurring uranium from vaporized sediment [13]; however, both of these sources had natural U isotopic abundances ($^{235}U/^{238}U = 0.00725$). The $^{235}U/^{238}U$ ratios of Trinity glasses do not vary systematically over the sampled volatility range and most measurements are indistinguishable from the natural $^{235}U/^{238}U$ (Fig. 4). This result demonstrates that U isotopes did

not experience resolvable mass-dependent fractionation during the Trinity explosion. The mass difference between ^{235}U and ^{238}U is small (1.3%) but similar to mass differences between many fissiongenic and non-fissionogenic isotopes – e.g., ^{90}Sr vs. ^{88}Sr (2.2%), ^{99}Mo vs. ^{98}Mo (1.0%), ^{137}Cs vs. ^{133}Cs (2.9%). We conclude that mass-dependent isotopic fractionation was limited for elements above ~90 a.m.u., and thus that heavy stable isotopes are reliable volatility (chemical) proxies for fissionogenic isotopes.

In his seminal paper on the phenomenon of fractionation in fallout debris, Freiling[6] scaled fractionation using a ratio of the most and least refractory measured fissionogenic radionuclides ($^{95}Zr/^{89}Sr$). Logarithmic fractionation trends first demonstrated by Freiling[6] are reproduced for Trinity debris using both the major-element volatility index and a ratio of stable trace-element proxies (Th/Rb) to scale fractionation (Fig. 5; Supporting Information). Freiling[6] estimated cumulative weighted volatilities for entire fissionogenic decay chains based on experimental data to develop an empirical relationship between fractionation and volatility. Fractionation scaling with the major-element volatility index bypasses the need for such an estimate and allows for development of a volatility scale specific to the conditions and environmental composition of a given explosion. Moreover, the magnitude of fractionation observed through microanalysis of Trinity glasses is comparable to that observed in bulk samples over four different tests[6]. This result demonstrates that radionuclide volatility and fractionation in a nuclear explosion can be reliably determined from small volumes of compositionally heterogeneous glassy fallout without measurement of specific fissionogenic radionuclides. Thus, stable trace elements can provide detailed information about fireball conditions, a vital step in the forensic reconstruction of a nuclear device and its effects.

References

(1) Fahey, A. J.; Zeissler, C. J.; Newbury, D. E.; Davis, J.; Lindstrom, R. M. *P. Natl. Acad. Sci.* **2010**, *107* (47), 20207–20212.

(2) Mayer, K.; Wallenius, M.; Varga, Z. *Chem. Rev.* **2013**, *113* (2), 884–900.

(3) Hutcheon, I. D.; Grant, P. M.; Moody, K. J. Vertes, A., Nagy, S., Klencsar, Z., Lovas, R. G., Eds.; Handbook of Nuclear Chemistry, 2011; pp 2837–2891.

(4) Lewis, L. A.; Knight, K. B.; Matzel, J. E.; Prussin, S. G.; Zimmer, M. M.; Kinman, W. S.; Ryerson, F. J.; Hutcheon, I. D. *J. Environ. Radioact.* **2015**, *148*, 183–195.

(5) Adams, C. E.; Farlow, N. H.; Schell, W. R. *Geochim. Cosmochim. Ac.* **1960**, *18* (1), 42–56.

(6) Freiling, E. C. *Science* **1961**, *133* (3469), 1991–1998.

(7) Belloni, F.; Himbert, J.; Marzocchi, O.; Romanello, V. *J. Environ. Radioact.* **2011**, *102* (9), 852–862.

(8) Cassata, W. S.; Prussin, S. G.; Knight, K. B.; Hutcheon, I. D.; Isselhardt, B. H.; Renne, P. R. *J. Environ. Radioact.* **2014**, *137*, 88–95.

(9) Wallace, C.; Bellucci, J. J.; Simonetti, A.; Hainley, T.; Koeman, E. C.; Burns, P. C. *J. Radioanal. Nucl. Ch.* **2013**, *298* (2), 993–1003.

(10) Bellucci, J. J.; Simonetti, A.; Koeman, E. C.; Wallace, C.; Burns, P. C. *Chem.Geol.* **2014**, *365*, 69–86.

(11) Freiling, E. C.; Crocker, G. R.; Adams, C. E. Klement, A. W., Ed.; Radioactive fallout from nuclear weapons tests: Germantown, MD, 1965; pp 1–41.

(12) Eppich, G. R.; Knight, K. B.; Jacomb-Hood, T. W.; Spriggs, G. D.; Hutcheon, I. D. *J.*

Radioanal. Nucl. Ch. **2014**, *302* (1), 593–609.
(13) Bellucci, J. J.; Simonetti, A.; Wallace, C.; Koeman, E. C.; Burns, P. C. *Anal. Chem.* **2013**, *85* (8), 4195–4198.
(14) Eby, G. N.; Charnley, N.; Pirrie, D.; Hermes, R.; Smoliga, J.; Rollinson, G. *Am. Mineral.* **2015**, *100* (2-3), 427–441.
(15) Bonamici, C. E.; Kinman, W. S.; Fournelle, J. H.; Zimmer, M. M.; Pollington, A. D.; Rector, K. D. *Contrib. Mineral. Petrol.* **2017**, *172* (1), 2.
(16) Stewart, K. *Transactions of the Faraday Society* **1956**, *52*, 161–173.
(17) Weisz, D. G.; Jacobsen, B.; Marks, N. E.; Knight, K. B.; Isselhardt, B. H.; Matzel, J. E.; Weber, P. K.; Prussin, S. G.; Hutcheon, I. D. *Geochim. Comsochim. Ac.* **2017**, *201*, 410–426.
(18) Smith, D. K.; Williams, R. W. *J. Radioanal. Nucl. Ch.* **2005**, *263* (2), 281–285.
(19) Sharp, N.; McDonough, W. F.; Ticknor, B. W.; Ash, R. D.; Piccoli, P. M.; Borg, D. T. *J. Radioanal. Nucl. Ch.* **2014**, *302* (1), 57–67.
(20) Lodders, K. *The Astrophysical Journal* **2003**, *591*, 1220–1247.
(21) Allègre, C.; Manhès, G.; Lewin, É. *Earth Planet. Sc. Lett.* **2001**, *185* (1), 49–69.
(22) McDonough, W. F.; Sun, S. S. *Chemical Geology* **1995**, *120* (3), 223–253.
(23) Glasstone, S.; Dolan, P. J. *The Effects of Nuclear Weapons*, 3rd ed.; U.S. Department of Defense, 1977.
(24) Hanson, S. K.; Pollington, A. D.; Waidmann, C. R.; Kinman, W. S.; Wende, A. M.; Miller, J. L.; Berger, J. A.; Oldham, W. J.; Selby, H. D. *P. Natl. Acad. Sci.* **2016**, *113* (29), 8104–8108.
(25) Hervig, R. L.; Mazdab, F. K.; Williams, P.; Guan, Y.; Huss, G. R.; Leshin, L. A. *Chem. Geol.* **2006**, *227* (1-2), 83–99.
(26) Pearce, N. J. G.; Perkins, W. T.; Westgate, J. A.; Gorton, M. P.; Jackson, S. E.; Neal, C. R.; Chenery, S. P. *Geostand. Geolanal. Res.* **2007**, *21* (1), 115–144.
(27) Jochum, K. P.; Weis, U.; Stoll, B.; Kuzmin, D.; Yang, Q.; Raczek, I.; Jacob, D. E.; Stracke, A.; Birbaum, K.; Frick, D. A.; Günther, D.; Enzweiler, J. *Geostand. Geoanal. Res.* **2011**, *35* (4), 397–429.
(28) Kita, N. T.; Ushikubo, T.; Bin Fu; Valley, J. W. *Chem. Geol.* **2009**, *264* (1-4), 43–57.
(29) Ranebo, Y.; Hedberg, P. M. L.; Whitehouse, M. J.; Ingeneri, K.; Littmann, S. *J. Anal. Atom. Spectrom.* **2009**, *24* (3), 277–287.
(30) Zimmer, M.; Kinman, W.; Kara, A.; Steiner, R. *Minerals* **2014**, *4* (2), 541–552.
(31) Anders, E.; Grevesse, N. *Geochim. Cosmochim. Ac.* **1989**, *53* (1), 197–214.
(32) Koeman, E. C.; Simonetti, A.; Chen, W.; Burns, P. C. *Anal. Chem.* **2013**, *85* (24), 11913–11919.
(33) Lamoreaux, R. H.; Hildenbrand, D. L.; Brewer, L. *J. Phys. Chem. Ref. Data* **1987**, *16* (3), 419–443.
(34) Miller, C. F. *A Theory of Formation of Fallout from Land-surface Nuclear Detonations and Decay of the Fission Products*; USNRDL-TR-425; U.S. Naval Radiological Defense Laboratory, 1960; pp 1–119.
(35) *CRC Handbook of Chemistry and Physics*, 84 ed.; Lide, D. R., Ed.; CRC Press, 2004; pp 1–2475.
(36) Yoneda, S.; Grossman, L. *Geochim. Cosmochim. Ac.* **1995**, *59* (16), 3413–3444.
(37) Ebel, D. S. Lauretta, D. S., McSween, H. Y., Eds.; Meteorites and the earth solar system II, 2006; pp 253–277.

(38) Bainbridge, K. T. *Trinity*; LA-6300-H; Los Alamos Scientific Laboratory, 1976; p 82.

Acknowledgements
CB thanks Drs. Warren Oldham and Susan Hanson for providing samples. This project was funded through the United States Department of Energy National Nuclear Security Administration, the Glenn T. Seaborg Institute for Actinide Science, and the Strategic Outcomes Office of Los Alamos National Laboratory. This publication has been cleared for unlimited release under LA-UR-16-XXXX.

Conflict of Interest Disclosure
The authors declare no competing financial interests.

Supporting Information. Additional background information and data tables
Bonamicietal_SupportingInfo.docx. Background on volatility index and Freiling data
Bonamicietal_SupportingInfo_DataTables.xlxs. Trace-element and U-Pb isotope data

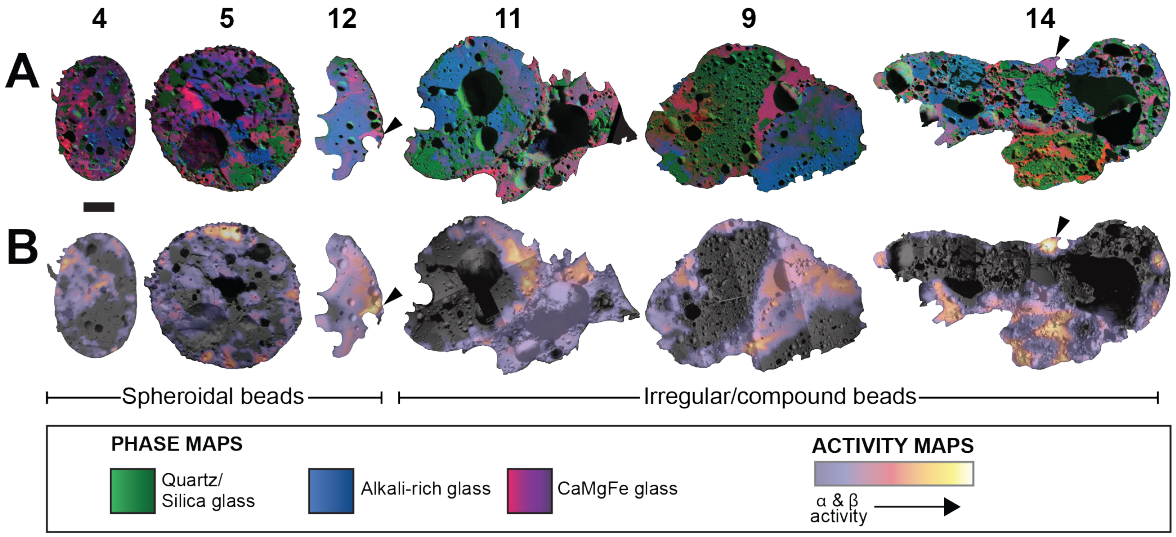

Figure 1. Maps of glassy fallout debris from the Trinity nuclear test. (A) Phase maps showing variations in major-element composition of glass phases. (B) Activity maps showing variations in the concentration of (present-day) radioactive trace elements. Activity correlates with glasses formed by condensation from the fireball plasma[15]. Arrows indicate domains of refractory-element-rich glass.

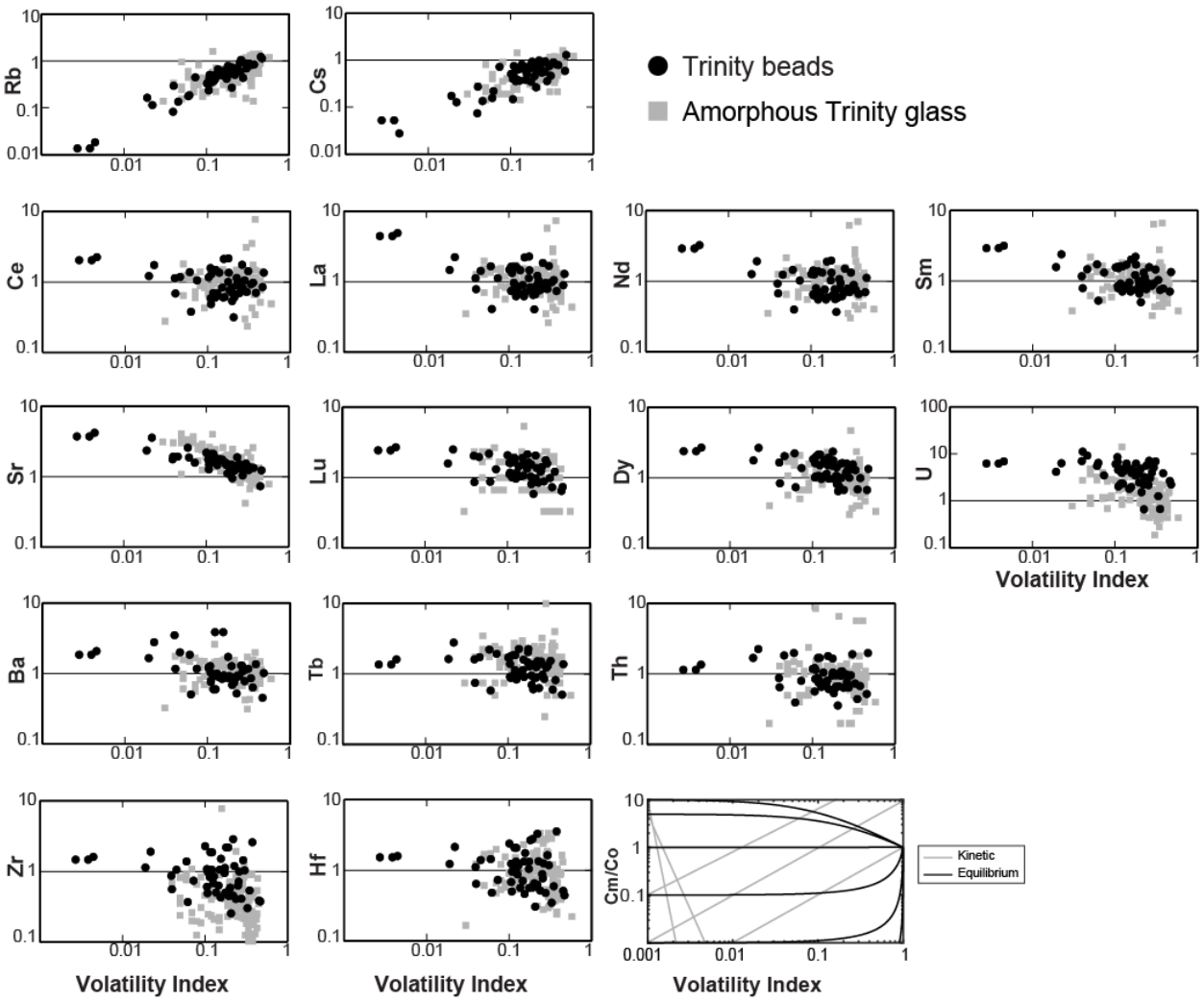

Figure 2. Trace element concentrations as a function of major-element volatility index. Element concentrations are normalized to the element concentration measured in Trinity test site sediment[10]. Graphs are arranged in order of decreasing volatility from top to bottom and from left to right within each row as determined by comparison of trace-element ratios. Black dots are concentrations measured in spheroidal beads of this study. Gray boxes are concentrations measured in glassy crusts[10]. Lowest right shows ideal modeled kinetic (Rayleigh) and equilibrium fractionation trends for comparison with actual trace element trends. Cm/C_0 denotes the ratio of concentration in condensed melt to concentration in initial fireball vapor. For both types of models, incompatible element concentrations increase with increasing volatility index, whereas compatible element concentrations decrease with increasing volatility index.

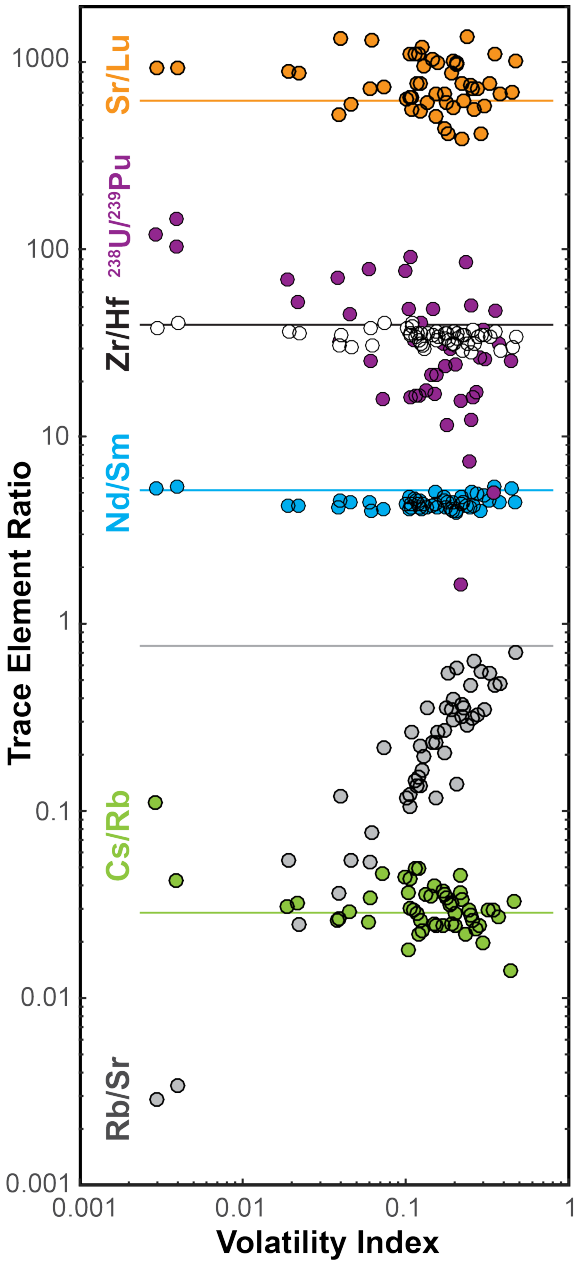

Figure 3. Trace-element ratios as a function of volatility index. Horizontal lines indicate the trace-element ratio in bulk Trinity test-site sediment[10] for comparison.

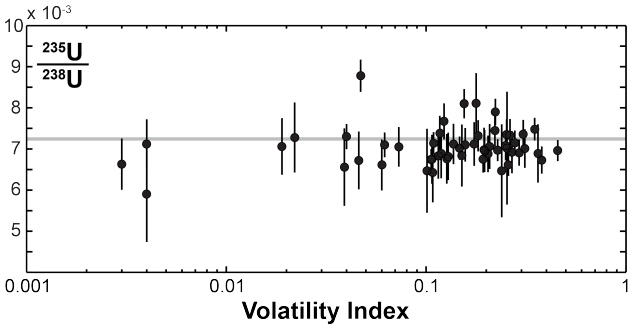

Figure 4. Uranium isotope ratio as a function of volatility index. Horizontal gray line indicates the initial, natural U isotopic composition of the Trinity tamper[38] and the test-site sediment. Error bars show 2SD uncertainties.

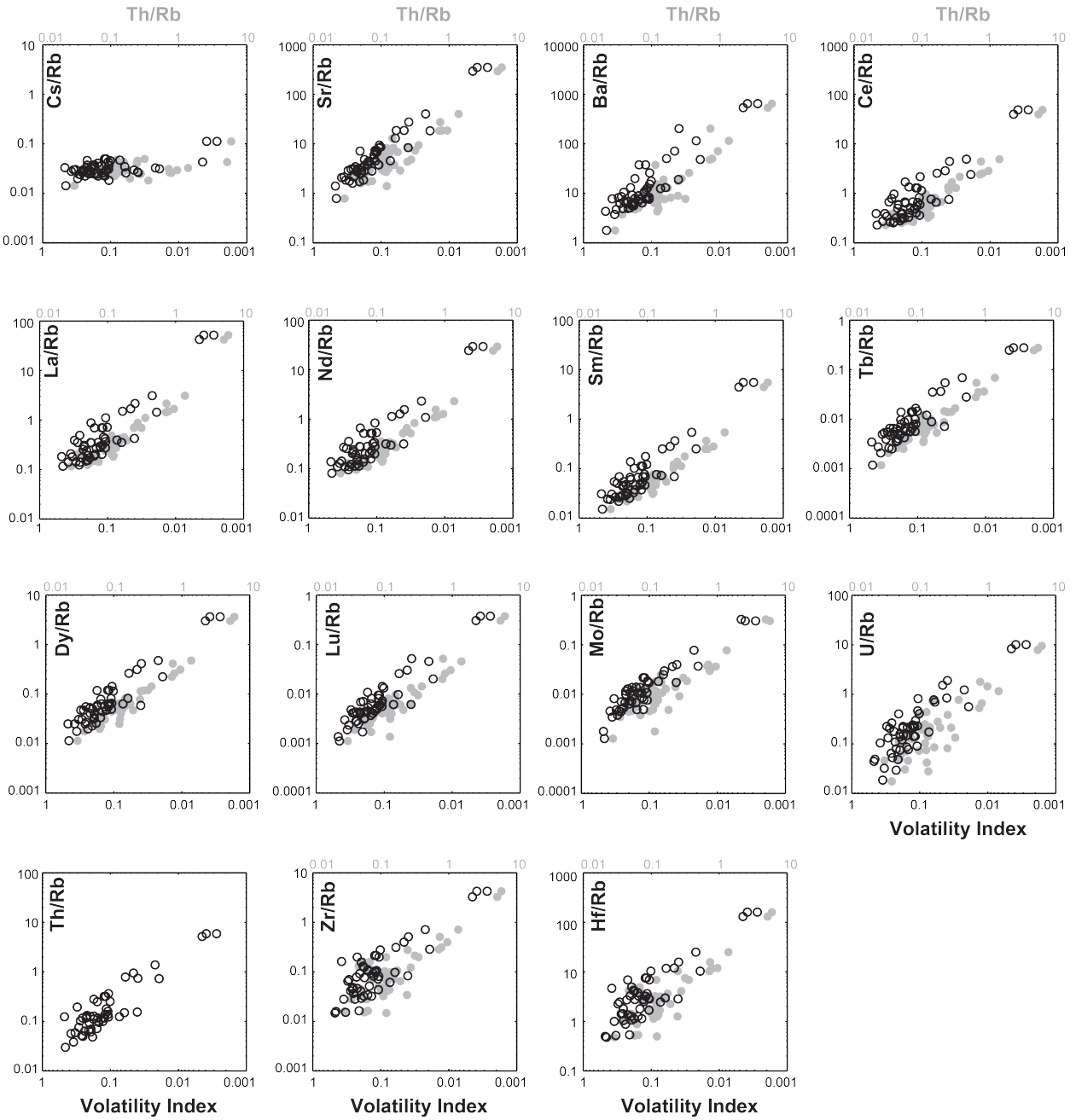

Figure 5. Trace element ratios in trinitite glasses plotted as a function of Th/Rb (closed gray symbols, top scale) and major-element volatility index (open black symbols, bottom scale). Logarithmic trends are comparable to those documented by Freiling[6] for bulk debris from four deep-water or near-surface coral atoll tests. The absolute slopes of these trends are dominated by the variation in Rb abundance, which is much greater than abundance variations of other measured trace element (except Cs). Note that the Volatility Index axis has been reversed (refractory to the right, volatile to the left) relative to Figs. 2-4 in order to mimic the scale of Freiling[6].

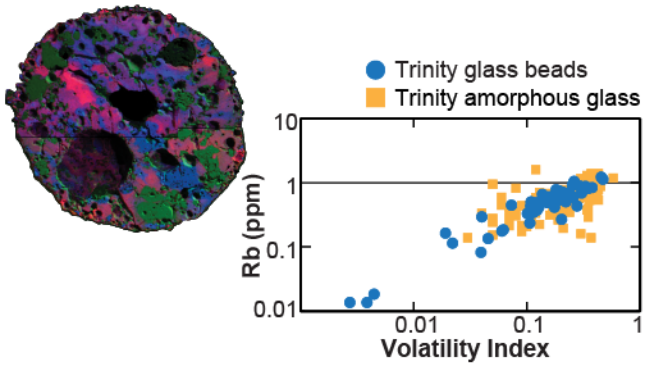
Trinity glass beads
Trinity amorphous glass
Rb (ppm)
10
1
0.1
0.01
0.01
0.1
1
Volatility Index

For TOC only

Supporting Information

Article: Tracking radionuclide fractionation in the first atomic explosion using stable elements

Authors & Affiliations:
Chloë E. Bonamici, Nuclear and Radiochemistry Group, Chemistry Division, Los Alamos National Laboratory, PO Box 1663, MS J514, Los Alamos, NM, 87545, USA

Richard L. Hervig, School of Earth and Space Exploration, Arizona State University, PO Box 871404, Tempe, AZ, 85287, USA

William S. Kinman, Nuclear and Radiochemistry Group, Chemistry Division, Los Alamos National Laboratory, PO Box 1663, MS J514, Los Alamos, NM, 87545, USA

This document contains graphics showing the origin of the major-element volatility index and a comparison of relative condensation order of elements. It also contains a brief background discussion of the fractionation trends first documented by Freiling (1961). Trace-element and U-Pu-isotope data are tabulated in a separate Excel file as Tables S-1 and S-2.

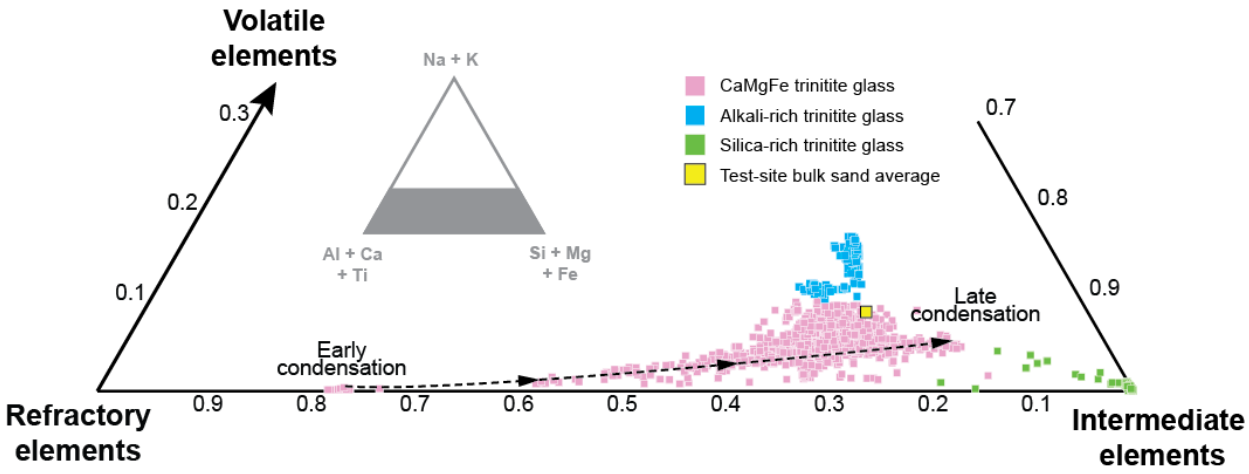

Figure S-1. Ternary compositional diagram showing the relative volatility of trinitite glasses. CaMgFe trinitite glasses, which formed by condensation, define an approximately linear trend from early-formed refractory-element-enriched glasses toward later-formed, intermediate- and volatile-element-enriched glasses. Alkali-rich and silica-rich trinitite glasses formed by melting of Trinity test-site minerals. Modified from Bonamici et al.[15].

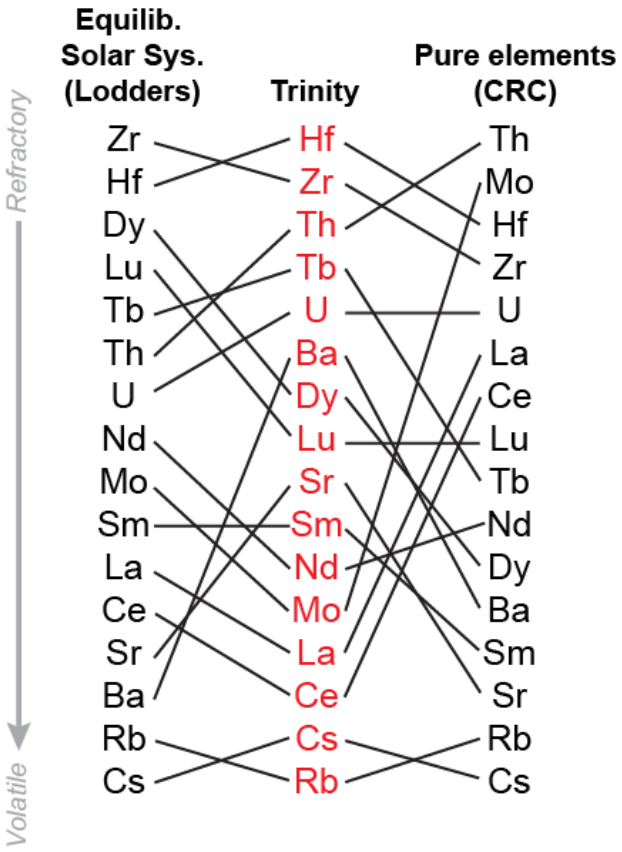

Figure S-2. Comparison of relative condensation order of elements in Trinity glassy fallout debris, the early solar system, and pure-element experiments. Condensation order for elements in Trinity glasses are inferred from trace-element ratios (e.g., Ba/Nd, Ce/La, Zr/Th, etc.) as a function of major-element volatility index. Condensation order for elements in the early solar system is based on equilibrium thermodynamic calculations for a system with a composition similar to that of CI chondrites[20]. Condensation order for pure elements is based on experimentally determined boiling points of pure elements at 1 atmosphere (101.325 kPa) pressure[35]. With the exception of Sr and Ba, the Trinity glasses show a condensation order more similar to that calculated for the early solar system than determined for pure elements. This is consistent with the idea that the starting fireball plasma composition is a significant control on condensation order of elements in fallout debris, and that the fireball composition resembles the device surroundings, which in the case of Trinity, were primarily natural silicates materials.

Freiling (1961) Fractionation Trends

Freiling demonstrated the control of volatility on fractionation of fissionogenic nuclides using the fission ratio of nuclides expected to have very different volatilities (^{95}Zr and ^{89}Sr) as a scale. The fission ratio (f_i/f_j) is the measured atomic abundance divided by the per-fission yield of each nuclide. Freiling reasoned that the disparate volatilities of Zr and Sr would make this ratio particularly sensitive to fractionation.

Trace-element ratios plotted in Figure 5 are mass abundance ratios, rather than fission ratios, but are nonetheless comparable to the fission ratios of Freiling. Elements and isotopes measured for this study were nonfissionogenic and thus fission ratios could not be calculated. However, because the fission yields are constant factors, fission ratios are directly proportional to measured atom ratios. Similarly, conversion of measured isotope abundances from atom abundance (ppm atomic) to mass abundance (ppm weight) requires introduction of constant factors, such that mass abundance ratios are directly proportional to atom ratios.

Th/Rb was chosen for comparison with the major-element volatility index scale. This trace-element ratio is similar to the Zr/Sr ratio of Freiling because Th was among the most refractory-behaving elements during the Trinity explosion and Rb was among the most volatile. Zr/Sr was not used because Sr was relatively refractory-behaving element in the Trinity explosion, based on strong fractionation of Rb and Sr and weak fractionation of elements like Sr and Lu.